

## Modeling Heat Transfer through CRUD

Dong Yeol Yeo<sup>a</sup>, Hee Cheon NO<sup>a\*</sup>

<sup>a</sup>KAIST, Department of Nuclear and Quantum Engineering, 291 Daehak-ro, Yuseong-gu, Daejeon 34141

\*Corresponding author: hcno@kaist.ac.kr

### 1. Introduction

One of the challenges we face in light water reactor is to maintain a comparative advantage over other energy systems in terms of cost. The most important issues with this tasks is to use high burnup fuel and to uprate power of reactors. Recently, many light water reactors uprated their rated power. However, for these reactors, the accelerated deposition of corrosion product on fuel rods has been problem. Researchers found that the increased reactor power had initiated the sub-cooled boiling on the upper portion of the core, and it accelerates the deposition of the corrosion products. The corrosion product layer attached to the fuel rod is called CRUD.

One of the major phenomena induced by CRUD is CRUD induced power shift (CIPS). CIPS is the phenomenon in which uneven deposition of CRUD causes distortion in the designed power distribution. The liquid flow that forms when boiling occurs in the CRUD draws boron in the coolant into the CRUD pores. As a result, the boron builds up in the CRUD. Because boron is a strong absorber of neutrons, it reduces the neutron flux used in fission reactions. Eventually, this leads to distortion of the power distribution.

Interestingly, this phenomenon is closely related to CRUD heat transfer. Understanding mechanism through which the CRUD conducts heat transfer over various power ranges of the nuclear fuel rods will contribute to predicting the risk of this phenomenon.

Heat transfer characteristics of CRUD have been studied experimentally by some researchers. Experiments performed at the Westinghouse Advanced Loop Tester (WALT) are representative among CRUD heat transfer experiments [1]. This experiment obtained boiling curves for various CRUDs under simulated PWR conditions. The experiment's researchers of this experiment obtained the effective thermal conductivities ( $k_{eff}$ ) of CRUDs through experiment, and they found that the thermal conductivity is strongly dependent on the heat fluxes. They argued that boiling increased the heat transfer capability of CRUD at first, and that the further increase of heat flux could degrade heat transfer capability via increased vapor fraction.

On the other hand, the CRUD heat transfer model has been proposed by many researchers [2-5]. Most of these studies follow the concept proposed by P. Cohen [2]. He estimated that wick boiling of CRUD occurred because of the evaporation on the lateral wall of the steam chimney. This model extends into a variety of forms by adopting a two-dimensional shape [3], adopting chemical transfer and reaction [4], or adopting convection terms in heat transfer equations [5]. Most of

the models deal with the nucleate boiling regime and do not go beyond this regime.

In this paper, the heat transfer characteristics of CRUD along heat fluxes will be discussed. The database from WALT was carefully analyzed to identify the heat transfer regimes in CRUD. Furthermore, the heat transfer model for boiling regimes, which are crucial for CIPS phenomenon, were introduced.

### 2. Heat Transfer Regimes

This section describes the method used to identify heat transfer regimes of CRUD, and identified heat transfer regimes are introduced.

#### 2.1 Method

Heat transfer regimes were identified using boiling curves in the WALT database [1]. It is assumed that the change in the heat transfer regime would lead to the change in the dependency of heat flux on the wall superheat. In other words, the boiling curves in a certain regime can be expressed as below.

$$q \sim \Delta T^n, \quad (1)$$

where  $n$  changes with heat transfer regime.

#### 2.3 Heat Transfer Regimes

Analysis on boiling curves revealed that there were five heat transfer regimes for CRUD. The characteristics of these regimes are described both in graphical description (Fig.1) and in boiling curve (Fig.2).

The first regime was the liquid-saturated regime (A in Fig.2). For this regime, since only the liquid fills the pores of the CRUD, the  $k_{eff}$  of CRUD can be obtained using following relationship:

$$k_{sl} = k_s(1 - \phi) + k_l\phi. \quad (2)$$

Here,  $k_s$  and  $k_l$  is liquid and solid thermal conductivity, and  $\phi$  is the porosity of the CRUD.

The nucleate boiling regimes (B and C in Fig.2) were followed after the liquid-saturated regime. The previous work of the present author found that the liquid supply for the nucleate boiling was limited to that from capillarity of the CRUD [6]. In this case, the exponent  $n$  of (Eq.1) became 0.75. We named this regime as capillary nucleate boiling (Capillary NB) regime (C in Fig.2). Before Capillary NB regime, we found that some

boiling curve had higher exponent than capillary NB regime. An order of exponent was between two and three, which is similar to those observed from the bare surface nucleate boiling. Therefore, we concluded that the demand for liquid was so small that the required supply was not limited by the capillarity. We called this regime as uninhibited NB (Uninhibited regime, B in Fig.2).

When the liquid supply was not enough to fulfill the demand from the heated surface, the dryout occurred. The dryout flux for the CRUD did not mean the critical heat flux (CHF), since the dryout did not lead to the sudden increase of temperature. Instead, the vapor would slowly grow along the heat fluxes. In this regime, the vapor film was confined in the CRUD, thus it was named as confined film boiling regime (D in Fig.2). The vapor grew with increasing heat flux, thus the boiling curve in this regime followed the expression below.

$$q = k_{sv} \frac{\Delta T}{\delta_v} \quad (3)$$

where  $k_{sv}$  is the  $k_{eff}$  for the vapor-filled CRUD, and  $\delta_v$  is the vapor film thickness. When vapor film grew, the larger wall superheat or heat flux resulted in thicker film. As a result,  $n$  of (Eq.1) for this regime became less than one.

The CHF would be reached when the vapor film was suddenly spilled over from the CRUD. In a certain condition, the liquid supply would be not enough to confine the vapor film within the CRUD. As a result, the vapor film could be spilled over the CRUD, and the thermal resistance from the fuel rod to the coolant would suddenly increase. To confirm this scenario, the simple analysis on thermal resistance degradation for this regime was conducted. The wall superheat for confined FB regime was estimated using (Eq.3), and that for spilled-over FB regime was estimated assuming there was 1  $\mu\text{m}$  vapor film above the CRUD.

$$q = \left( \frac{l_{CRUD}}{k_{sv}} + \frac{1\mu\text{m}}{k_v} \right)^{-1} \Delta T \quad (4)$$

where  $l_{CRUD}$  is the thickness of CRUD.

The result is shown on Fig.3. The resistance suddenly increased as the vapor film was spilled over. Increased resistance might contribute to the overheating of fuel rod surface, and this might lead to the failure of fuel rod. For WALT database, this regime was not observed.

### 3. Capillary Nucleate Boiling Model

Among suggested heat transfer regimes, Capillary NB regime is closely related to the CIPS. In this section, the heat transfer model for this regime will be introduced.

#### 3.1 Model Description

The model for capillary NB regime was suggested by these authors [6]. In this paper, it was assumed that the

phase change mechanism during the boiling regime was due to the nucleate boiling at the CRUD-clad interface rather than the evaporation at the lateral wall of the steam chimney. This assumption was supported by a visual observation of bubble nucleation on a heater substrate in a heat pipe experiment with a wick structure similar to CRUD [7].

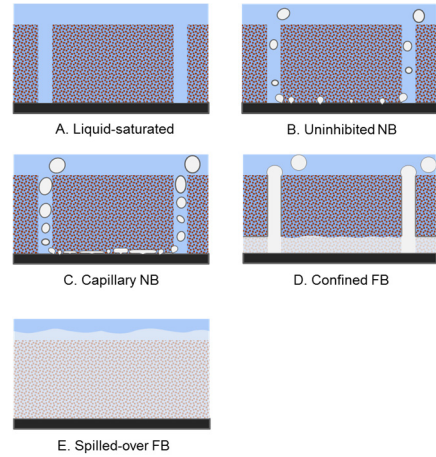


Fig. 1. Schematic description of five heat transfer regimes of CRUD.

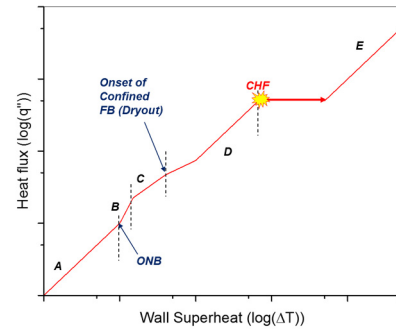


Fig. 2. Five heat transfer regimes on boiling curve for CRUD.

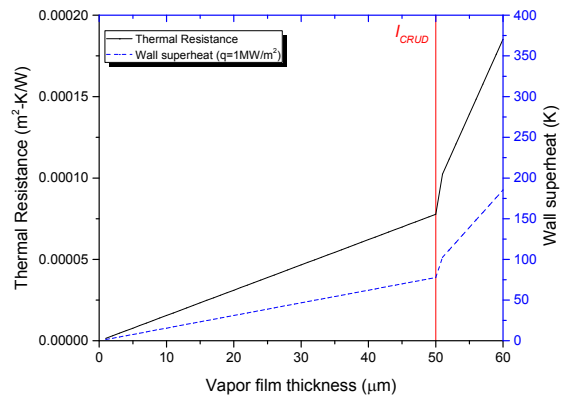


Fig. 3. Simple analysis on thermal resistance for confined FB regime (regime D), and spilled-over FB regime (regime E). Typical PWR condition ( $P=15.5\text{MPa}$ ,  $q=1\text{MW/m}^2$ ) and CRUD ( $l_{CRUD} = 50\mu\text{m}$ ,  $\phi = 0.5$ ) is used for analysis.

In this model, total heat applied from the bottom of the CRUD was partitioned into three parts: these were (1) nucleate boiling in the thermal boundary layer (TBL), (2) convective heat removal by subcooled liquid flow within CRUD, and (3) forced convective heat removal at the CRUD-coolant interface.

At first, the heat transferred from the CRUD-clad interface was partially removed by the nucleate boiling in TBL. The form of pool boiling correlation suggested by Foster and Zuber was used to describe the nucleate boiling in TBL [8].

$$q_b = C_{\beta,m} \Delta T_{sat}^{2m+0.75} \quad (5)$$

Here  $C_{\beta,m}$  is constant determined by empirical constants  $\beta$ ,  $m$  and fluid properties.

$$C_{\beta,m} = \frac{\beta \pi^{m-0.5}}{\sqrt{2}} \left( \frac{\rho_f^{2n-0.75} c_{pf}^{n-0.167} k_{sl}^{n+0.167} v_{fg}^{2n-1.75}}{\mu_f^{n-0.333} h_{fg}^{2n-1.75} \sigma^{0.5} T_{sat}^{0.75}} \right) \quad (6)$$

The empirical constants were found by comparing models result to the WALT database. It was found that the least sum of squares of deviations was reached when  $\beta$  and  $m$  are 0.00061 and 0, respectively.

The next step was to find the thickness of TBL. Because the TBL thickness was very thin ( $\sim 5 \mu\text{m}$ ), the linear temperature distribution within TBL could be assumed. This resulted in the following relationship for the wall superheat and the TBL thickness ( $l_{TBL}$ ).

$$q_w = k_{sl} \left. \frac{dT}{dx} \right|_w = k_{sl} \frac{\Delta T_{sat}}{l_{TBL}} \quad (7)$$

After heat was firstly removed by the nucleate boiling, the heat was transferred to the wick region where pores are fully saturated with liquid flows. In this region, the differential equation for energy balance (Eq.8-A) was solved with two boundary conditions (Eq.8-B and C).

$$\frac{d}{dx} \left( \alpha_{sl} \frac{dT}{dx} \right) = u_f \frac{dT}{dx} \quad , \quad (8-A)$$

$$s \alpha_{sl} \left. \frac{dT}{dx} \right|_{x=0} = \frac{h_o}{\rho_f c_{pf}} (T(0) - T_b) \quad , \quad (8-B)$$

$$s \alpha_{sl} \left. \frac{dT}{dx} \right|_{x=l-TBL} = \frac{q_w - q_b}{\rho_f c_{pf}} \quad , \quad (8-C)$$

where  $\alpha_{sl}$  is thermal diffusivity for liquid-filled CRUD ( $\alpha_{sl} = k_{sl}/\rho_f c_{pf}$ ),  $s$  is fraction of area that is not covered by chimneys,  $u_f$  is liquid velocity assuming all liquid inflow is changed into vapor by boiling heat ( $u_f = q_b/\rho_f h_{fg} s$ ),  $h_o$  is the forced convective heat transfer coefficient for bulk flow, and  $T_b$  is the bulk fluid temperature. Solving above equation gave the following relationship for  $q_b$  and  $l_{TBL}$ .

$$\Delta T_{sub} = (q_w - q_b) \left[ \frac{1}{h_o} e^{-\frac{u_f}{\alpha_{sl}}(l-l_{TBL})} + \frac{h_{fg}}{q_b c_{pf}} \left\{ 1 - e^{-\frac{u_f}{\alpha_{sl}}(l-l_{TBL})} \right\} \right] \quad (9)$$

As a result, we finally have three equations [(Eq.5), (Eq.7) and (Eq.9)] and three variables [ $q_b$ ,  $\Delta T_{sat}$ , and  $l_{TBL}$ ]. Therefore, we can solve the system of equations to find wall superheat ( $\Delta T_{sat}$ ).

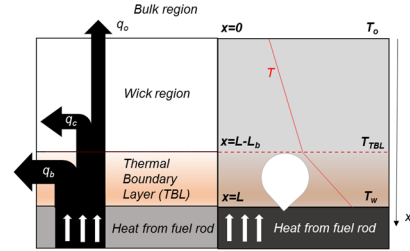


Fig. 4. Schematic description of CRUD heat transfer during capillary NB regime.

### 3.2 Results and Discussion

The model was validated to the WALT database [6]. Firstly, the data was selected so that only nucleate boiling regime was included in the database. The prediction capability of the model was estimated by comparing overall heat transfer coefficient (HTC), which was defined as below.

$$U_o = \frac{q_w}{T_w - T_b} \quad (10)$$

In other researches, the  $k_{eff}$  was usually used as the parameter for heat transfer performance of the CRUD [1-2,5]. However, the CRUD-coolant interface temperature should be known to obtain this parameter. In an experiment, the CRUD-coolant temperature cannot be measured because the CRUD grows during the experiment, and because it is difficult to install measurement device at this interface. Therefore, researchers have to infer the CRUD-coolant interface temperature using their own methodology. For example, in the WALT report, they conducted the same experiment both for clean surface and for the surface with CRUDs, and they obtained the  $k_{eff}$  of CRUD by comparing thermal resistances from two experiments [1]. However, their assumption is valid only when heat is transferred to the coolant only via a serial conduction. This is not true because heat can be transferred to the coolant through more than one mechanism: this can be either nucleate boiling or forced convection at the CRUD-coolant interface. In this case, the overall HTC in which directly measured values are used is proper choice for the validation and comparison.

Fig. 5 shows the result of the validation. The result from Cohen's model is shown together to compare its

prediction capability to ours. The prediction from our model was within the  $\pm 20\%$  bounds comparing to the measured values, while that from Cohen's model showed large deviations in low subcooling cases. The normalized root mean square error of the present model was 18.6%, while that of Cohen's model was 42.4%.

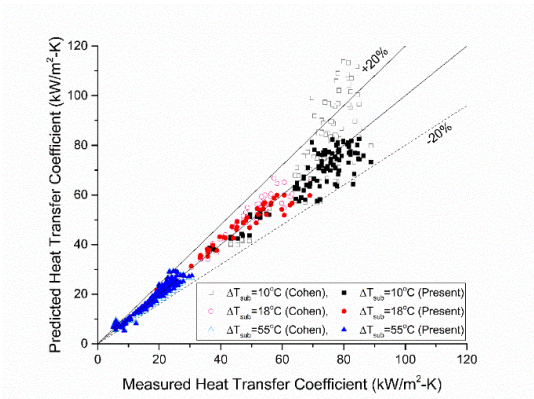


Fig. 5. Validation of the suggested model with the WALT database [6].

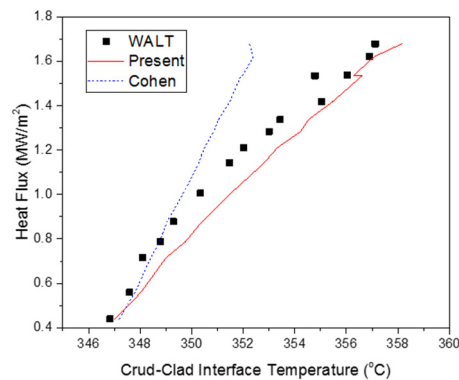


Fig. 6. Boiling curve for ROD-80 of WALT database [1] and prediction results from the present and Cohen's model.

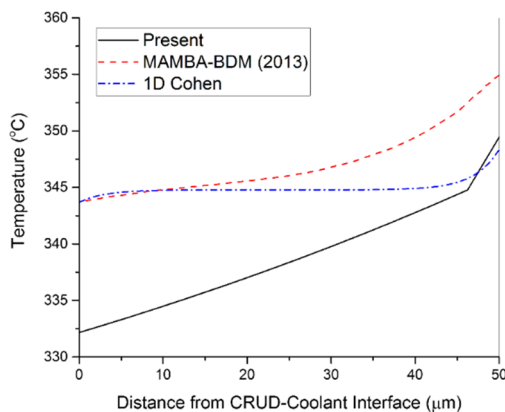


Fig. 7. Temperature distribution along the depth of CRUD. The result from the suggested model is compared to those of 1-D Cohen model and MAMBA-BDM [6].

Fig. 6 shows the boiling curve obtained for low subcooling case (ROD-80 of WALT database, 10°C subcooling). Comparing to Cohen's model, the present

model predicted larger wall superheat for same heat flux, and it was more close to the observed boiling curve. This difference comes from the phase change mechanism. In the case of Cohen's model, the phase change was occurred along the lateral wall of steam chimney, thus the uniform temperature region existed in the CRUD as shown in Fig. 7. On the other hand, in the present model, the phase change was occurred at the CRUD-clad interface, thus, there was no uniform temperature region within the CRUD.

#### 4. Conclusions

Heat transfer mechanism of the CRUD was carefully investigated using the WALT Database, which was the simulated PWR condition experiment for the CRUD heat transfer. Firstly, by analyzing the boiling curves of the database, the heat transfer regimes for the CRUD were identified. It was found that there were five regimes, which were the liquid-saturated regime, the uninhibited NB regime, the capillary NB regime, the confined FB regime, and the spilled-over FB regime. Among these regimes, model for the capillary NB regime was suggested, since this regime is closely related to the CIPS. This model was compared to the WALT database, and it showed normalized RMSE of 18.6%, while the previous model (Cohen model) showed the RMSE of 42.4%. This enhancement seemed to be mainly achieved by adopting CRUD-clad interface nucleate boiling as phase change mechanism, rather than adopting the chimney wall evaporation.

#### REFERENCES

- [1] Simulated Fuel Crud Thermal Conductivity Measurement Under Pressurized Water Reactor Conditions, EPRI, Palo Alto, CA: 2011. 1022896.
- [2] P. Cohen, Heat and Mass Transfer for Boiling in Porous Deposits with Chimneys, AIChE symposium series, Vol.70, p. 71, 1974.
- [3] I. ul Haq, N. Cinosi, M. Bluck, G. Hewitt, and S. Walker, Modelling heat transfer and dissolved species concentrations within PWR crud, Nuclear Engineering and Design, Vol.241, p. 155, 2011.
- [4] J. Henshaw, J. C. McGurk, H. E. Sims, A. Tuson, S. Dickinson, and J. Deshon, A model of chemistry and thermal hydraulics in PWR fuel crud deposits, Journal of Nuclear Materials, Vol.353, p. 1, 2006.
- [5] M. Short, D. Hussey, B. Kenderick, T. Besmann, C. Stanek, and S. Yip, Multiphysics modeling of porous CRUD deposits in nuclear reactors, Journal of Nuclear Materials, Vol.443, p. 579, 2013.
- [6] D.Y.Yeo and H.C.NO, Modeling heat transfer through chimney-structured porous deposit formed in pressurized water reactors, International Journal of Heat and Mass Transfer, Vol.108, p.868, 2017.
- [7] J.A.Weibel and S.V.Grimella, Visualization of vapor formation regimes during capillary-fed boiling in sintered-powder heat pipe wicks, International Journal of Heat and Mass Transfer, Vol.55, p.3498, 2012.
- [8] H. Foster and N.Zuber, Dynamics of vapor bubbles and boiling heat transfer, AIChE J. 1, p.531, 1955